JMEPEG (2010) 19:1290–1297
DOI: 10.1007/s11665-010-9611-7

1059-9495/$19.00

Constitutive Equation and Processing Map for Hot Deformation of SiC Particles Reinforced Metal Matrix Composites

Peng Zhang, Fuguo Li, and Qiong Wan

(Submitted June 29, 2009; in revised form November 29, 2009)

Flow behavior and microstructures of Al/15% SiCp were investigated by hot compression tests using Gleeble-1500 thermomechanical simulator at temperatures ranging from 440 to 500 °C with strain rates of 0.001-1.0 s^{-1}. The high-temperature deformation behaviors of Al/15% SiCp were analyzed based on the true stress-true strain curves. The results show that the softening mechanism at low strain rate (0.001 s^{-1}) is dynamic recovery, and at high strain rates (0.01, 0.1, and 1 s^{-1}) is dynamic recrystallization (DRX). Based on these experimental data, a set of constitutive equations for Al/15% SiCp are described by the Zener-Hollomon parameter, and the coefficients of equations are found to be functions of strain. The constitutive equations reveal the dependence of flow stress on strains, strain rates, and temperatures. Furthermore, the mean error between the experimental and the calculated flow stress was computed. The result shows that the calculated results from constitutive equations are in good agreement with the experimental results. To demonstrate the potential workability of Al/15% SiCp, the processing map was established. The stable zones and the instability zones in processing map are identified and verified through micrographs. As a result, the optimum strain rates and temperatures for effective hot working of Al/15% SiCp were determined.

Keywords constitutive equation, hot deformation, metal matrix composites, processing map

1. Introduction

Discontinuously particles reinforced metal matrix composites (MMC) are recognized as an important class of engineering material due to their lightweight and superior mechanical and thermal properties (Ref 1-4). However, the MMC exhibits poor ductility at room temperature due to the presence of brittle ceramic particles (Ref 5, 6). Further studying has found that the MMC can be formed by thermomechanical processing (Ref 7-9). In order to obtain favorable microstructure and required properties, better control of forming processes is rather essential. The results show that the flow behavior of composite is in direct correlation with the strain rates, temperatures, and deformation degree (Ref 10, 11). Therefore, the optimization of the technical parameters will become complicated. In recent years, the finite element method (FEM) offers a good opportunity to figure out this difficulty (Ref 12-14). And the progress in computer hardware and software has enabled complicated simulations of industrial forming processes. Nevertheless, the accuracy of such simulations will remain dependent on the reliability of the material data, especially the correlation between true stress and true strain at different deformation conditions. Generally, the experimental tests at different strains, strain rates, and temperatures during metal forming process are performed to reveal this constitutive relationship, such as tension, compression, and torsion (Ref 15). Now, the data needed for the constitutive relationship can be obtained by thermo-mechanical compression test. It is well known that the compression test is a convenient approach for achieving large deformation response of metals and the advantage of this method is easy to prepare the specimens (Ref 16-18). Additionally, the test process is similar to the forging process. Therefore, the data obtained from the compression test can depict the flow behavior of metals during forming. As a result, considerable investigations based on the compression tests have been performed in order to establish flow stress relationships of materials during hot deformation.

In this paper, isothermal compression of Al/15% SiCp has been conducted at different strain rates and hot working temperatures. Based on these experimental data, a set of constitutive equations incorporating the effects of strains, strain rates, and temperatures were established to describe the plastic flow properties. Also, the reliability of the constitutive equations was evaluated by the mean error between the experimental and the calculated flow stress. Furthermore, the approach of processing map has been introduced to study the deformation mechanisms and to optimize hot forming process for this material. These maps show the stable and unstable deformation in the processing space on the axes of temperatures and strain rates. It is helpful to understand the interaction effects between strain rates and temperatures. Consequently, the components with controlled microstructure and properties can be manufactured without macro or micro defects.

Peng Zhang and **Fuguo Li**, School of Materials Science and Engineering, Northwestern Polytechnical University, Xi'an 710072, China; and **Qiong Wan**, Hennan University of Science and Technology, Luoyang 471003, China. Contact e-mails: nsdi@mail.nwpu.edu.cn and fuguolx@nwpu.edu.cn.

2. Experimental Procedure

The material (aluminum alloy reinforced by 15% SiC particles with size 10-15 μm) was made by a powder metallurgy route. Cylindrical specimens were machined from the as-received materials with diameter of 8 mm and height of 12 mm for uniaxial compression tests. The original microstructure is shown in Fig. 1. It is obvious that the microstructure exhibits marked band distribution. Also, it is found that in some locations, the particles distributed with clustering. In order to investigate the deformation behavior of composites, the hot deformation tests were performed using Gleeble-1500 thermomechanical simulator at temperatures from 440 to 500 °C and strain rates from 0.001 to 1.0 s^{-1}. As soon as compression tests terminated, the specimens were quenched in water in order to preserve the hot deformed microstructure. Then, the deformed specimens were sectioned vertically and microstructure investigation was carried out using light optical microscope (OM), as shown in Fig. 2. Figure 2 presents the typical microstructure of hot deformed Al/15% SiCp composites samples. It is clear that the original microstructures have been replaced by recrystallized structure, which can be attributed to the occurrence of dynamic recrystallization (DRX) (Ref 19, 20). Traditionally, DRX is a beneficial process in hot deformation since it not only gives a stable flow and good workability to the materials by simultaneously softening but also reconstitutes the microstructure (Ref 21).

Typical true stress-true strain curves obtained during hot deformation are given in Fig. 3. At high strain rates (0.01, 0.1, and 1 s^{-1}) the flow stress reaches a peak at a critical strain and then sharply decreases to a steady value at different temperatures. The characteristics of this flow stress curves demonstrate the happening of DRX. Generally, DRX is a beneficial process in hot deformation since it not only gives stable flow and good workability to the material by simultaneously softening it but also reconstitutes the microstructure. At low strain rate (0.001 s^{-1}), the curves reach a maximum and then almost attain the near steady state with increase of strain, which indicates the occurrence of dynamic recovery. Therefore, it is observed that the flow stress is in direct correlation with the strain rates. The variation of stress is related to a variation in dislocation density as well as the formation and development of subgrain boundaries, which result from working hardening and softening mechanism. At lower strain rates, the deformation is isothermal but at high strain rates it is adiabatic (Ref 22). This phenomenon at higher strain rate deformation is the consequence of the inadequate heat dissipation. Further, this leads to an increase in work hardening rate at higher strain rate deformation. However, at lower strain rate, the strain hardening is almost compensated by softening due to higher temperature. Hence, near steady state flow curve is observed. Moreover, another obvious difference among these curves is the slope of the elastic part of the curves. From these curves, it is evident that the slope of the elastic part of the curves at lower temperature (440 °C) at the same strain rate is the great when compared with other higher temperatures (460, 480, and 500 °C). The fact showed the intensity of the material at low temperature at the same strain rate is higher than that at high temperature. From the mentioned flow stress-strain character, it can be concluded that the work-hardening effect is pronounced at low temperatures. Generally, during the deformation the matrix around the SiC particles presents much higher dislocation density than that of normal alloy. The high dislocation density regions restrict the plastic flow and contribute to a competing behavior between dynamic softening and the work hardening, which can be expressed by constitutive equation concerning the deformation parameters. For this purpose, by using the experimental data obtained, the constitutive equation is introduced to describe the hot deformation behavior of composites.

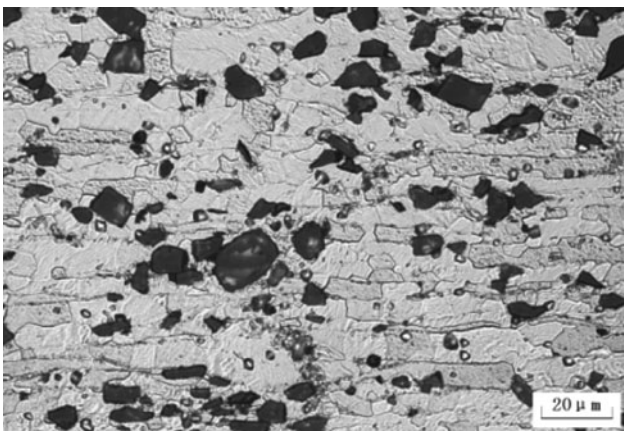

Fig. 1 Original microstructure of Al/15% SiCp

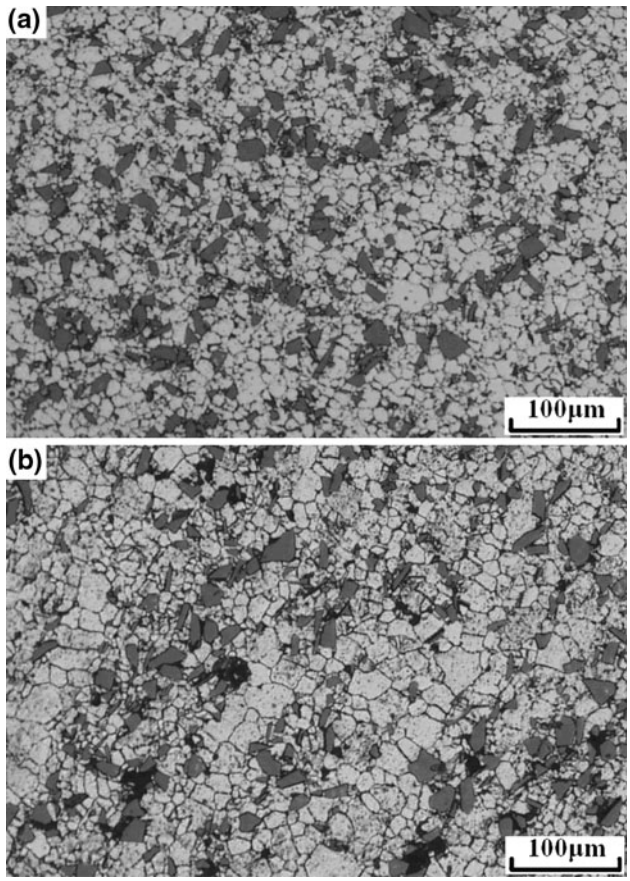

Fig. 2 Microstructure of Al/15% SiCp at (a) $T = 480$ °C, $\dot{\varepsilon} = 0.1$ s^{-1}; (b) $T = 500$ °C, $\dot{\varepsilon} = 0.01$ s^{-1}

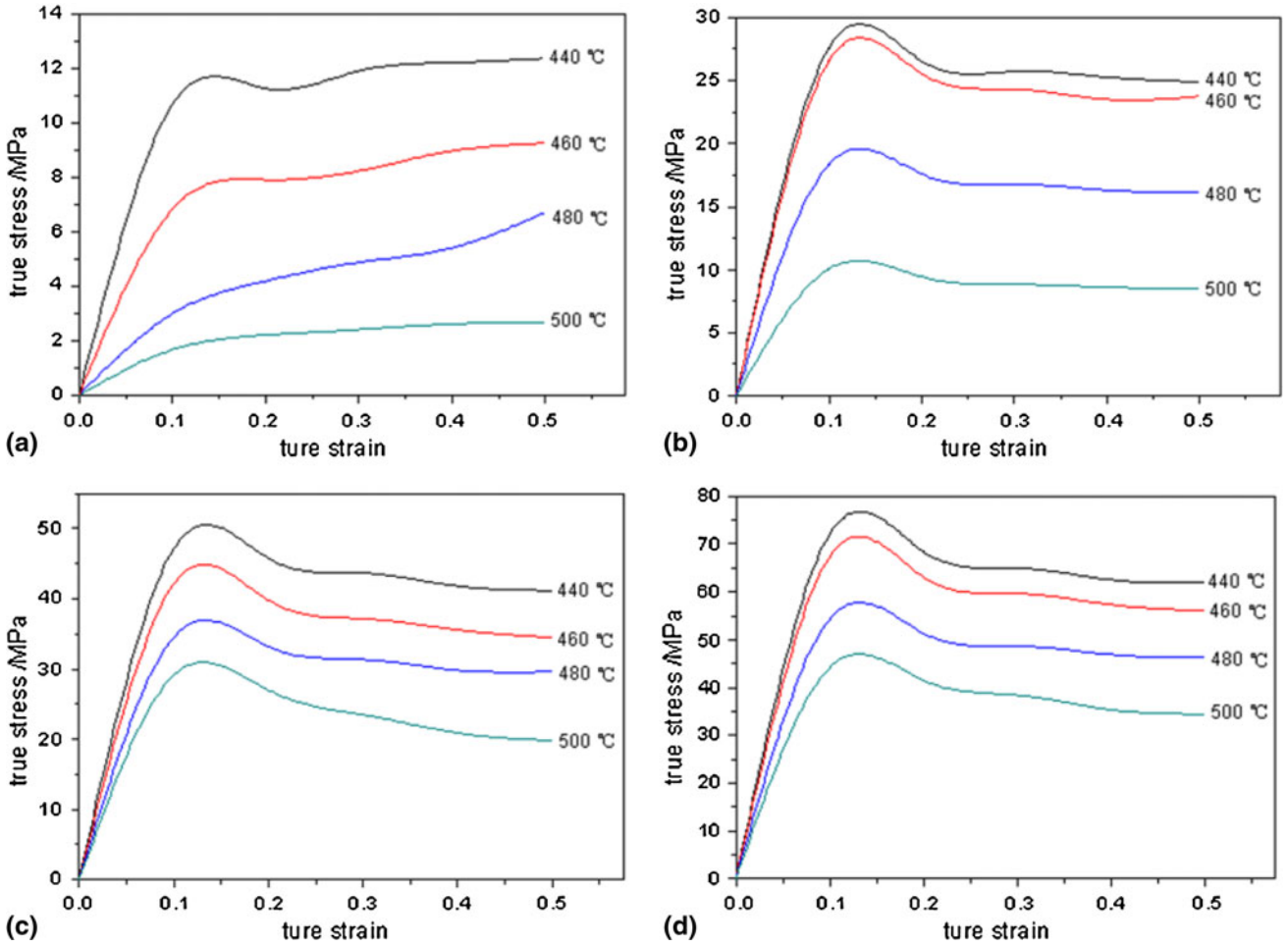

Fig. 3 Flow behavior of composites during hot compression deformation: (a) $\dot{\varepsilon} = 0.001\ s^{-1}$; (b) $\dot{\varepsilon} = 0.01\ s^{-1}$; (c) $\dot{\varepsilon} = 0.1\ s^{-1}$; (d) $\dot{\varepsilon} = 1\ s^{-1}$

3. Results and Discussion

3.1 Constitutive Equation

In hot deformation, the dependence of flow stress on the strain rate and temperature can be expressed as follows (Ref 16, 23):

$$\dot{\varepsilon} = A\phi(\sigma)\exp\left(-\frac{Q}{RT}\right) \quad \text{(Eq 1)}$$

where A is constant, Q is the activation energy of deformation (kJ/mol), R is the gas constant (kJ/mol K^{-1}), T is absolute deformation temperature (K), $\phi(\sigma)$ can be represented by constitutive models (Ref 18, 23).

$$\phi(\sigma) = \begin{cases} A'\sigma^n & \alpha\sigma < 0.8 \\ A''\exp(\beta\sigma) & \alpha\sigma > 1.2 \\ A'''[\sinh(\alpha\sigma)]^n & \text{for all } \sigma \end{cases} \quad \text{(Eq 2)}$$

where A', A'', A''', n, β, α are constants, and $\alpha = \beta/n$ (Ref 24). The stress model ($\alpha\sigma < 0.8$) is suitable for low stress level, the stress model ($\alpha\sigma > 1.2$) is suitable for high stress level, and the hyperbolic sine law is a more general form suitable for over a wide range (Ref 24).

For the purpose of determining the constitutive model for $\phi(\sigma)$, three key parameters (n, β, α) need to be obtained, respectively. For the low stress level and high stress level, the $\phi(\sigma)$ in Eq 1 is substituted by power law and exponential law, respectively. Then gives

$$\dot{\varepsilon} = B\sigma^n\exp\left(-\frac{Q}{RT}\right) \quad \text{(Eq 3)}$$

$$\dot{\varepsilon} = B'\exp(\beta\sigma)\exp\left(-\frac{Q}{RT}\right) \quad \text{(Eq 4)}$$

where B and B' are the material constants.

Taking the logarithm of both sides in Eq 3 and 4, respectively, then gives

$$\ln\sigma = \frac{1}{n}\ln\dot{\varepsilon} + \frac{1}{n}\left(\frac{Q}{RT} - \ln B\right) \quad \text{(Eq 5)}$$

$$\sigma = \frac{1}{\beta}\ln\dot{\varepsilon} + \frac{1}{\beta}\left(\frac{Q}{RT} - \ln B'\right) \quad \text{(Eq 6)}$$

It is obvious that the value of n and β can be obtained from the slope of the lines in the $\ln\sigma - \ln\dot{\varepsilon}$ and $\sigma - \ln\dot{\varepsilon}$. The strain 0.5 is taken as an example to illuminate the process, as shown in Fig. 4 and 5. It can be seen that the correlation of $\ln\sigma - \ln\dot{\varepsilon}$ and $\sigma - \ln\dot{\varepsilon}$ can be expressed in linear form. As a result, the value of n and β can be obtained according to the slope of the lines.

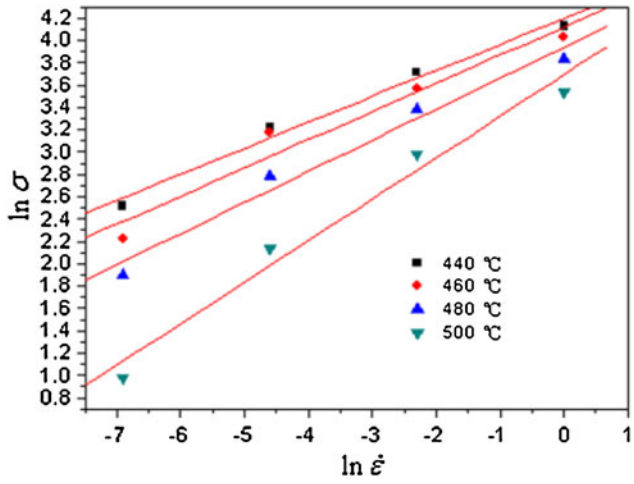

Fig. 4 Curves of $\ln\sigma - \ln\dot{\varepsilon}$

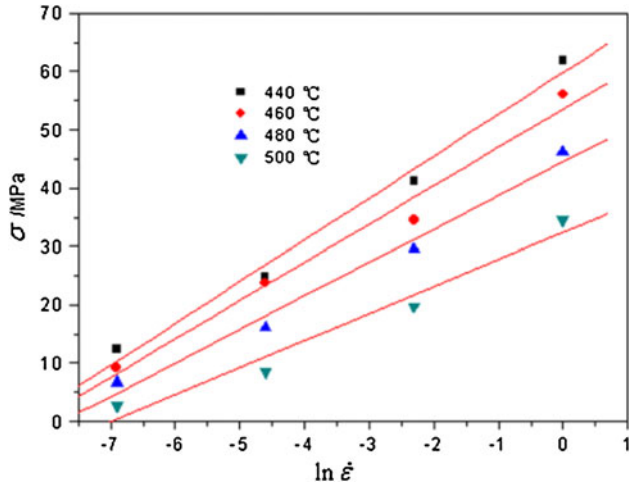

Fig. 5 Curves of $\sigma - \ln\dot{\varepsilon}$

Based on the method mentioned above, the parameters at strain 0.1, 0.2, 0.3, 0.4, and 0.5 are computed, respectively, as shown in Table 1. The variations product of parameter $\alpha\sigma$ with strain rate and temperature is shown in Table 2. From Table 2, it is evident that the maximum value of $\alpha\sigma$ is 3.39094, the minimum value of $\alpha\sigma$ is 0.08242. Consequently, the hyperbolic sine constitutive model is selected for describing the constitutive relationship, which can be written as

$$\dot{\varepsilon} = K[\sinh(\alpha\sigma)]^n \exp\left(-\frac{Q}{RT}\right) \quad \text{(Eq 7)}$$

Taking the logarithms of both sides in Eq 7 gives

$$\ln[\sinh(\alpha\sigma)] = -\frac{1}{n}\ln K + \frac{1}{n}\left(\frac{Q}{RT} + \ln\dot{\varepsilon}\right) \quad \text{(Eq 8)}$$

Here, the Zener-Hollomon parameter Z (temperature modified strain rate) (Ref 16, 23, 24) can be employed to characterize the combined effects of strain rate and temperature on the deformation process, as given in Eq 9:

$$Z = \dot{\varepsilon}\exp\left(\frac{Q}{RT}\right) \quad \text{(Eq 9)}$$

Taking the logarithms of both sides in Eq 9 gives

$$\ln Z = \ln\dot{\varepsilon} + \frac{Q}{RT} \quad \text{(Eq 10)}$$

Table 1 Values of three key parameters

	Strain				
	0.1	**0.2**	**0.3**	**0.4**	**0.5**
n	2.72853	2.91265	3.10974	3.29641	3.44341
β	0.12838	0.13908	0.15036	0.16088	0.16896
α	0.04705	0.04775	0.04835	0.0488	0.04907

Table 2 Values of $\alpha\sigma$ with strain rate and temperature

		Strain				
Temperature, °C	**Strain rate, s^{-1}**	**0.1**	**0.2**	**0.3**	**0.4**	**0.5**
440	0.001	0.50193	0.537	0.57488	0.57638	0.62123
	0.01	1.29952	1.26666	1.24376	1.21605	1.23946
	0.1	2.21723	2.18069	2.10908	2.03945	2.01943
	1	3.39094	3.26515	3.14077	3.04907	3.04008
460	0.001	0.32083	0.37727	0.39739	0.43725	0.45404
	0.01	1.25012	1.21939	1.17578	1.14646	1.16625
	0.1	1.98231	1.89706	1.79625	1.7345	1.69095
	1	3.16835	3.01236	2.88345	2.79463	2.75381
480	0.001	0.13983	0.19959	0.2358	0.26362	0.32892
	0.01	0.86374	0.83792	0.81093	0.79046	0.80627
	0.1	1.62497	1.58196	1.51461	1.454	1.45134
	1	2.55373	2.44829	2.35203	2.28491	2.29962
500	0.001	0.08242	0.10523	0.11626	0.12743	0.13048
	0.01	0.47313	0.44985	0.4265	0.41407	0.42269
	0.1	1.36953	1.28481	1.13371	1.01665	0.9709
	1	2.07712	1.97704	1.85456	1.72288	1.69095

Then, substituting the corresponding item of Eq 8 gives

$$\ln[\sinh(\alpha\sigma)] = -\frac{1}{n}\ln K + \frac{1}{n}\ln Z \qquad C = -\frac{1}{n}\ln K \quad D = \frac{1}{n} \qquad \text{(Eq 11)}$$

Consequently, the linear relationship between stress and Z value is given in Eq 12:

$$\ln[\sinh(\alpha\sigma)] = C + D\ln Z \qquad \text{(Eq 12)}$$

In the present work, the relationship curves between stress and Zener-Hollomon parameter at strains ranging between 0.1

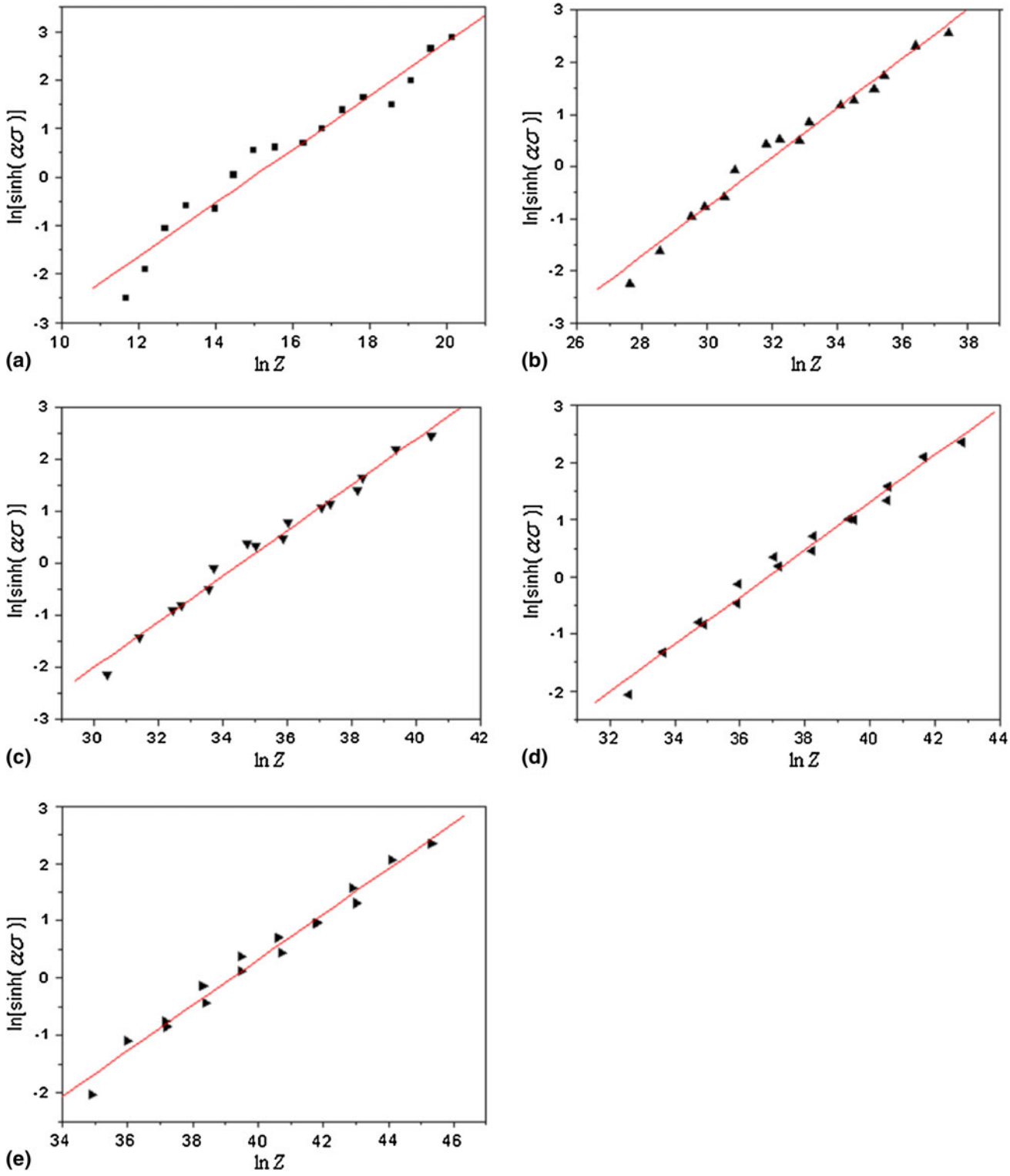

Fig. 6 Correlation between stress and Z parameter: (a) ε = 0.1; (b) ε = 0.2; (c) ε = 0.3; (d) ε = 0.4; (e) ε = 0.5

and 0.5 with an interval of 0.1 are shown in Fig. 6, respectively. According to theses fitting curves, the coefficients in Eq 12 can be obtained, as given in Table 3. From Table 3, it is obvious that the coefficients in Eq 12 are the functions of strain as shown by Eq 13 and 14.

Then, Eq 12-14 represent the constitutive equations for Al/15% SiCp at high temperature. It is evident that the flow stress of material investigated depends on strain, strain rate, and temperature:

$$C = 6.33803 - 200.319\varepsilon + 588.235\varepsilon^2 - 551.188\varepsilon^3 \quad \text{(Eq 13)}$$

$$D = 0.69239 - 1.765\varepsilon + 4.07\varepsilon^2 - 3.443\varepsilon^3 \quad \text{(Eq 14)}$$

Table 3 Coefficients in Eq 12

	Coefficient	
Strain	***C***	***D***
0.1	−8.28284	0.55376
0.2	−14.9254	0.47185
0.3	−15.21941	0.44013
0.4	−15.26761	0.41438
0.5	−15.58152	0.39751

By applying the determined coefficients in Table 2 to Eq 12, the flow stress values of composites at different deformation conditions can be calculated. Figure 7 shows the comparisons between the experimental and calculated flow stress values for the four tested strain rates under different temperatures, from which satisfactory agreement can be observed. In order to evaluate the accuracy of the established constitutive equations, mean error between the calculated and the experimental flow stress is calculated, and the value is 4.478%. The result demonstrates that the proposed deformation constitutive equations can provide an accurate estimate of the flow stress for Al/15% SiCp.

3.2 Processing Map

For bulk metal working processes, the knowledge of defining stable and unstable processing domains is very necessary. The ideal objective is to produce the product with required microstructure and properties, without macro or microstructure defects. Besides strain rate sensitivity m, another important parameter applied for investigating the hot deformation is power dissipation (η) (Ref 7, 9, 21, 22), which is explicitly expressed in terms of m based on power law assumption: $\eta = 2m/(m + 1)$. It is known from the test results on several materials that the maximization of η reduces the tendency of flow localization. The variation of η with strain

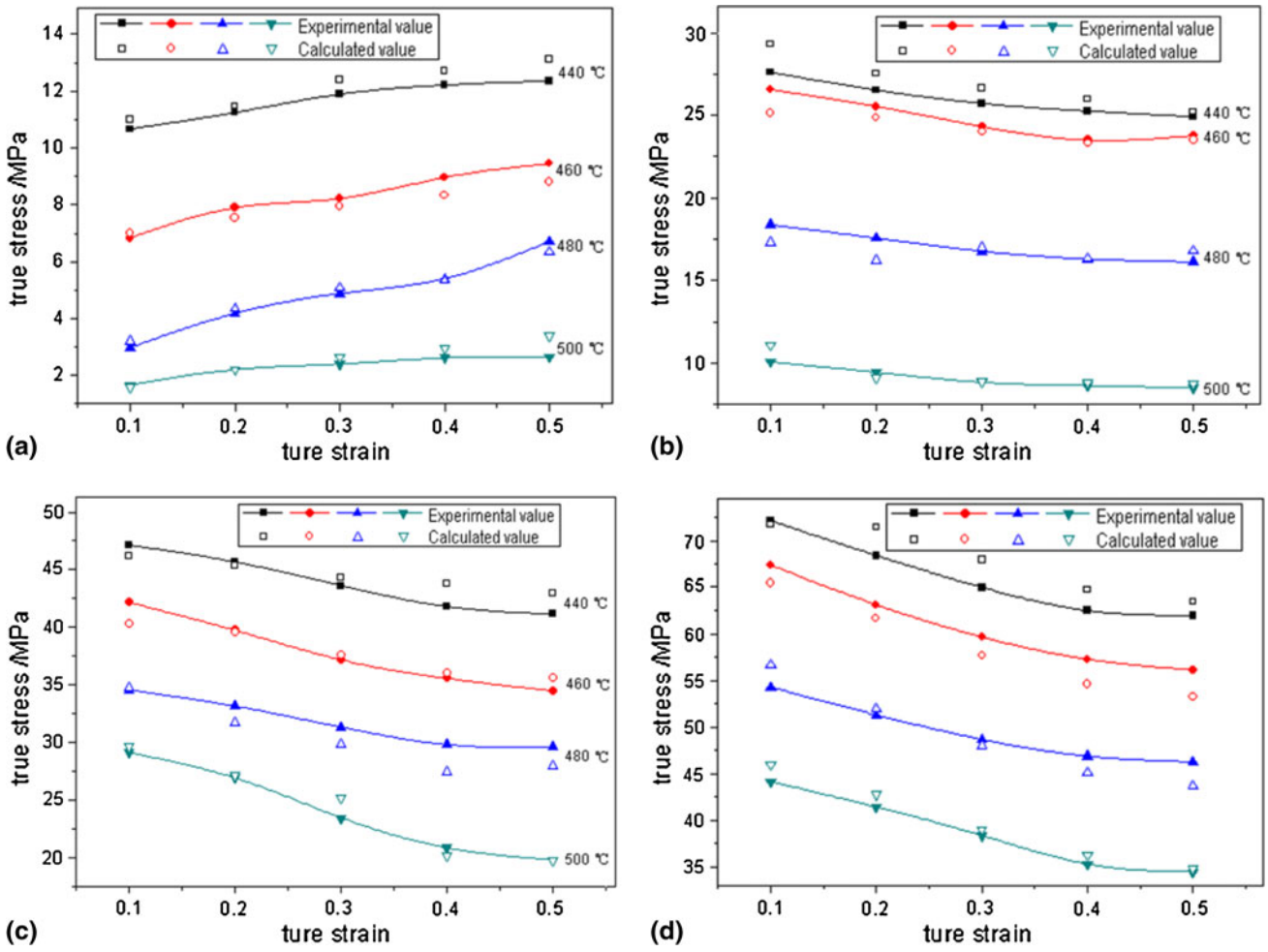

Fig. 7 Comparisons between the experimental and calculated flow stress: (a) $\dot{\varepsilon} = 0.001\ s^{-1}$; (b) $\dot{\varepsilon} = 0.01\ s^{-1}$; (c) $\dot{\varepsilon} = 0.1\ s^{-1}$; (d) $\dot{\varepsilon} = 1\ s^{-1}$

rates and temperatures at constant strain constitutes the power dissipation map, namely processing map, which can be used to depict the manner in which power is dissipated through microstructure change in deformation and hence reveals the emergence of fracture and instabilities. Generally, at low temperature and high strain rate, void formation occurs, while at high temperature and low strain rate, wedge cracking occurs at grain boundary triple junctions (Ref 25). At very high strain rate, instability due to adiabatic shear band formation is the likelihood (Ref 21). Here, in order to demonstrate the potential of the instability behavior, the instability criteria have been considered, defined as (Ref 8):

$$\frac{2m}{\eta} - 1 < 0 \qquad \text{(Eq 15)}$$

The processing map obtained for Al/15% SiCp composites at 0.5 strain is presented in Fig. 8. The contour numbers represent the power dissipation efficiency and the shaded domain indicates the regions of flow instability (negative flow instability parameters).

From Fig. 8, it can be seen that the processing map includes two typically stable domains. The first domain occurs in the range of 440-470 °C for a strain rates of 0.01738-0.1 s^{-1}. The maximum efficiency in this domain is 32%. This region is not recommended since the production rate is very low and the domain is rather narrow. The second domain occurs in the temperature range of 440-500 °C for wide strain rates of 0.001-0.01738 s^{-1}. The efficiency of this domain has increased from 38% to 68%. Microstructure analysis reveals that the original microstructure (Fig. 1) has been replaced by recrystallized structure (Fig. 2). Consequently, this domain can be interpreted to the effect of DRX. Generally, DRX is a beneficial process in hot deformation since it can produce stable flow. Thus, the DRX domain is often chosen for optimizing hot deformation and controlling the microstructure (Ref 22). However, Prasad and Seshacharyulu (Ref 25) proposed that DRX does not occur in aluminum and the primary softening mechanism is only dynamic recovery though exceptions have been made for very high-purity aluminum and some particle containing alloys. Though the basis for these conclusions has not been clearly understood, the presence of particles in aluminum can reduce the rate of dynamic recovery and shift the DRX domains to higher strain rates and temperature.

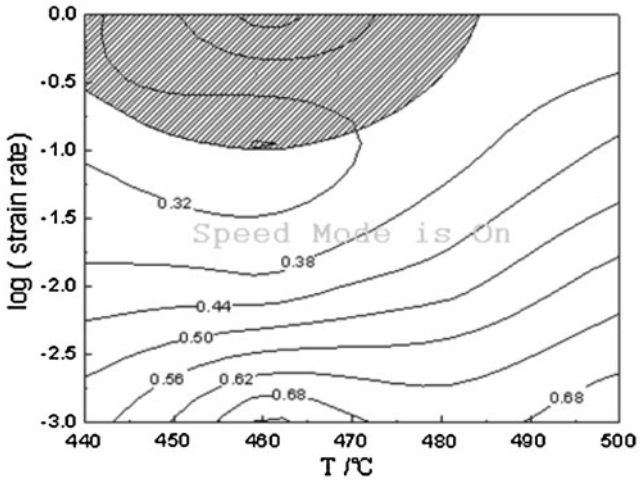

Fig. 8 Processing map at a strain of 0.5

The shaded domain in Fig. 8 represents the instability domain which occurs in the strain rates range of 0.1-1 s^{-1} between temperatures range of 440-480 °C. The structure in this domain is characterized by particle cracking and interface debonding due to flow localization as shown in Fig. 9 and 10. Localization usually occurs at peak load but sometimes it may occur before reaching peak. Beyond peak the material may experience softening or degradation in its load carrying capacity, but still continue to carry reduced load compared to peak load while growth and calescence of micro cracks continue during the falling region of the curve. Finally, the micro crack growth leads to a macro crack and fracture (Ref 22). At high strain rate the heat generation due to local temperature rise by plastic deformation is not easily conducted away, the flow stress in these deformation zones will decrease and further plastic flow will be localized (Ref 21, 22, 25). Furthermore, the presence of SiC particles in aluminum matrix causes the discontinuous deformation because the matrix undergoes plastic flow while the particles do not deform (Ref 14). As a result, the accumulated stress will emerge at the interface between the matrix and the particles. When the

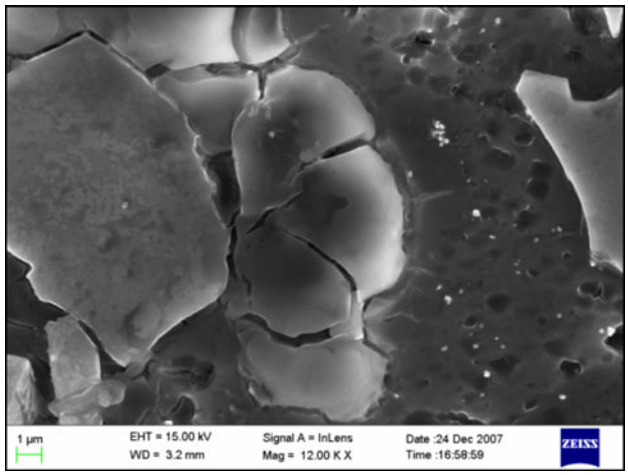

Fig. 9 Particle cracking

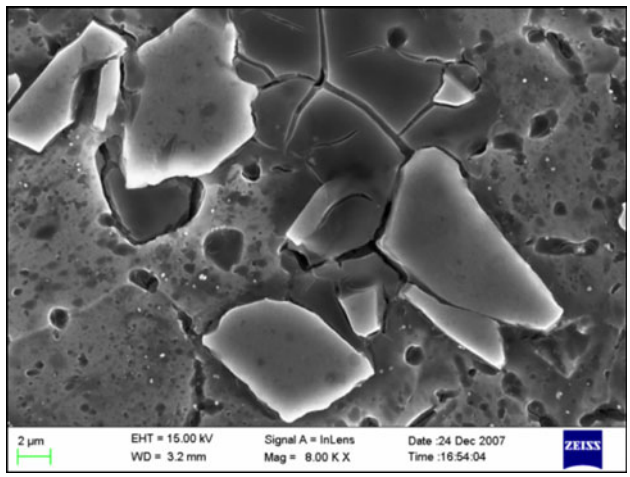

Fig. 10 Interface debonding

particle possesses tip, the accumulated stress will emerge in the vicinity of the particle tip, which may result in interface debonding or the particle itself cracking.

4. Conclusions

The mechanical behaviors of Al/15% SiCp were investigated with compression tests at temperatures ranging from 440 to 500 °C with strain rates of 0.001-1.0 s^{-1}. The basic conclusions can be drawn as follows:

1. During hot deformation the flow stress is in direct correlation with the strain rates. The softening mechanism at lower strain rate (0.001 s^{-1}) exhibits dynamic recovery behavior, and at high strain rates (0.01, 0.1, and 1 s^{-1}) exhibits dynamic recrystallization behavior.
2. A set of constitutive equations are established, in which the coefficients are functions of strains. Therefore, the constitutive equations reveal the dependence of flow stress on strain, strain rate, and temperature. Furthermore, the verification of constitutive equations shows good agreement with the experimental results.
3. The processing map is established to evaluate the efficiency of the forging process in the range of temperatures and strain rates investigated. The optimum domains and instability zone are obtained. The results show that dynamic recrystallization zone and superplastic zone are ideal to perform the hot deformation. In instability domain, the microstructures display particle cracking and interface debonding.

References

1. N. Chawla, X. Deng, and D.R.M. Schnell, Thermal Expansion Anisotropy in Extruded SiC Particle Reinforced 2080 Aluminum Alloy Matrix Composites, *Mater. Sci. Eng. A*, 2006, **426**, p 314–322
2. D.B. Miracle, Metal Matrix Composites—From Science to Technological Significance, *Compos. Sci. Technol.*, 2005, **65**, p 2526–2540
3. S. Basavarajappa and G. Chandramohan, Application of Taguchi Techniques to Study Dry Sliding Wear Behaviour of Metal Matrix Composites, *Mater. Des.*, 2007, **28**, p 1393–1398
4. S. Ramanathan, R. Karthikeyan, and G. Ganasen, Development of Processing Maps for 2124Al/SiCp Composites, *Mater. Sci. Eng. A*, 2006, **441**, p 321–325
5. D.P. Mondal, S. Das, and K.S. Suresh, Compressive Deformation Behaviour of Coarse SiC Particle Reinforced Composite: Effect of Age-Hardening and SiC Content, *Mater. Sci. Eng. A*, 2007, **460**, p 550–560
6. Z. Xue, Y. Huang, and M. Li, Particle Size Effect in Metallic Materials: A Study by the Theory of Mechanism-Based Strain Gradient Plasticity, *Acta Mater.*, 2002, **50**, p 149–160
7. G. Ganesan, K. Raghukandan, and R. Karthikeyan, Development of Processing Map for 6061 Al/15%SiCp Through Neural Networks, *J. Mater. Process. Technol.*, 2005, **166**, p 423–429
8. S.V.S. Narayana Murty, B. Nageswara Rao, and B.P. Kashyap, On the Hot Working Characteristics of 6061 Al-SiC and 6061-Al_2O_3 Particulate Reinforced Metal Matrix Composites, *Compos. Sci. Technol.*, 2003, **63**, p 119–135
9. E. Cerri, S. Spigarelli, and E. Evangelista, Hot Deformation and Processing Maps of Particulate-Reinforced 6061 + 20% Al_2O_3 Composite, *Mater. Sci. Eng. A*, 2002, **324**, p 157–161
10. K.S. See and T.A. Dean, The Effects of the Disposition of SiC Particles on the Forgeability and Mechanical Properties of Co-Sprayed Aluminium-Based MMCs, *J. Mater. Process. Technol.*, 1997, **69**, p 58–67
11. V.C. Srivastava, V. Jindal, and V. Uhlenwinkel, Hot-Deformation Behaviour of Spray-Formed 2014 Al + SiCp Metal Matrix Composites, *Mater. Sci. Eng. A*, 2008, **477**, p 86–95
12. S. Balasivanandha Prabu and L. Karunamoorthy, Microstructure-Based Finite Element Finite Analysis of Failure Prediction in Particle-Reinforced Metal-Matrix Composite, *J. Mater. Process. Technol.*, 2008, **207**, p 53–62
13. W.X. Zhang, T.J. Wang, and L.X. Li, Numerical Analysis of the Transverse Strengthening Behavior of Fiber-Reinforced Metal Matrix Composites, *Comput. Mater. Sci.*, 2007, **39**, p 684–696
14. Y.W. Yan, L. Geng, and A.B. Li, Experimental and Numerical Studies of the Effect of Particle Size on the Deformation of the Metal Matrix Composites, *Mater. Sci. Eng. A*, 2007, **448**, p 315–325
15. M. Poursina, H. Ebrahimi, and J. Parvizian, Flow Stress Behavior of Two Stainless Steels: An Experimental-Numerical Investigation, *J. Mater. Process. Technol.*, 2008, **199**, p 287–294
16. Z.P. Zeng, S. Jonsson, and Y. Zhang, Constitutive Equations for Pure Titanium at Elevated Temperatures, *Mater. Sci. Eng. A*, 2009, **505**, p 116–119
17. Y.L. Xiao, Q.L. Pan, and Y.B. He, Flow Behavior and Microstructural Evolution of Al-Cu-Mg-Ag Alloy During Hot Compression Deformation, *Mater. Sci. Eng. A*, 2009, **500**, p 150–154
18. Y. Wang, W.Z. Shao, and L. Zhen, Flow Behavior and Microstructures of Superalloy 718 During High Temperature Deformation, *Mater. Sci. Eng. A*, 2008, **497**, p 479–486
19. Z. Yang, Y.C. Guo, and J.P. Li, Plastic Deformation and Dynamic Recrystallization Behaviors of Mg-5Gd-4Y-0.5Zn-0.5Zr Alloy, *Mater. Sci. Eng. A*, 2008, **485**, p 487–491
20. X.M. He, Z.Q. Yu, and X.M. Lai, A Method to Predict Flow Stress Considering Dynamic Recrystallization During Hot Deformation, *Comput. Mater. Sci.*, 2008, **44**, p 760–764
21. G. Ganesan, K. Raghukandan, and R. Karthikeyan, Development of Processing Maps for 6061 Al/15% SiCp Composite Material, *Mater. Sci. Eng. A*, 2004, **369**, p 230–235
22. S. Ramanathan, R. Karthikeyan, and Manoj Gupta, Development of Processing Maps for Al/SiCp Composite Using Fuzzy Logic, *J. Mater. Process. Technol.*, 2007, **183**, p 104–110
23. H.E. Hu, L. Zhen, L. Yang, and W.Z. Shao, Deformation Behavior and Microstructure Evolution of 7050 Aluminum Alloy During High Temperature Deformation, *Mater. Sci. Eng. A*, 2008, **488**, p 64–71
24. Y.C. Lin, M.S. Chen, and J. Zhong, Constitutive Modeling for Elevated Temperature Flow Behavior of 42CrMo Steel, *Comput. Mater. Sci.*, 2008, **429**, p 470–477
25. P. Cavaliere, E. Cerri, and P. Leo, Hot Deformation and Processing Maps of a Particulate Reinforced 2618Al_2O_3/20p Metal Matrix Composite, *Compos. Sci. Technol.*, 2004, **64**, p 1287–1291